HEAT TRANSFER FROM BUBBLING POOLS

Progress Report

S. G. Bankoff - Principal Investigator (8.3%)

Anthony Luk - Research Assistant (50%)

Chemical Engineering Department

Northwestern University

Evanston, Illinois 60201

July 1, 1975 - October 1, 1975

PREPARED FOR THE U. S. ENERGY & RESEARCH DEVELOPMENT ADMINISTRATION UNDER CONTRACT NO. AT(11-1)-2554

DISCLAIMER

Task List

Task	Dates
1. Construct and debug rectangular pool Argonne boiling data	1/1/75 - 4/1/75
2. Series 1 - air - water at equivalent powers of 0 - 100 KW; heating and cooling	4/1/75 - 6/1/75
3. Series 2 - argon - water; heating and cooling	6/1/75 - 7/1/75
4. Series 3 - air - water in cylindrical geometry; heating and cooling	7/1/75 - 10/1/75
5. Series 4 - air - oil in cylindrical geometry; heating and cooling	10/1/75 - 12/1/75
6. Analysis of data and theoretical studies	6/1/75 - 2/1/76
7. Final report	3/1/76

Results

1. Progress on Tasks 1-3 and Task 5 and 6 are detailed in the accompanying report. The following changes may be noted:

    1. Heating experiments on a cold pool have not yet been performed, since this is considered to be of lower priority. Helium has been substituted for argon as the second gas in order to obtain a greater difference in gas densities. The air-oil information is still being collected ans is currently limited by air supply capacity.

2. Task 4

    The cylindrical pool has been constructed and data will be taken in the next month. No marked differences between the cylindrical and rectangular geometries are currently expected.

SIMULATION OF BOILING POOLS WITH INTERNAL HEAT SOURCES BY GAS INJECTION

S. G. Bankoff and Anthony C. H. Luk

Chemical Engineering Department
Northwestern University
Evanston, IL

ABSTRACT

It is shown that the heat transfer characteristics of volume-heated boiling pools can be successfully modeled by non-boiling pools with internal gas injection. The strong influence of spatial distribution of bubble sites is relevant to estimates of boiling fuel attack on gas-releasing sacrificial materials.

Presented at the Second Annual Post-Accident Heat Removal Information Exchange Meeting, Nov. 13-14, 1975, Albuquerque, N.M.

[1]Work supported by the U. S. Energy Research and Development Administration.

1. Introduction

A boiling fuel pool may exist in contact with sacrificial material for a relatively short time period immediately after core meltdown in a hypothetical reactor accident. This pool would be covered by a crust of solid fuel on top of which would lie molten steel. Clearly, the interaction between the two liquids can be quite strong if the fuel crust is thin and does not form an effective barrier. However, if the crust is thick enough to prevent effective liquid-liquid contact, the heat transfer at the bottom and sides of the pool will not be greatly affected by the heat transfer upwards to the solidified crust. In any case it is important to be able to estimate the extent of the attack on the sacrificial material in both horizontal and downward directions, since this will determine the evolution of the shape of the pool. Laboratory experiments with reactor materials are expensive, time-consuming and cannot be instrumented to give detailed information concerning heat transfer, in view of the extraordinary difficulties associated with boiling UO_2. In-pile experiments can be performed but are limited to small-diameter vessels. Since the fundamental lengths here are the average bubble diameter and the vessel diameter (or height), proper geometric scaling cannot be achieved unless the bubble diameter is much smaller than the characteristic length of the system. To achieve greater flexibility, simulant studies have been undertaken. Work at Argonne National Laboratory[1,2,3] has concentrated on heat transfer measurements from electrolytically-heated boiling aqueous salt solutions. These have shown that the downward heat transfer coefficient is substantially smaller

than the sideward heat transfer coefficient, and that the Nusselt number can be correlated in terms of a Reynolds number based upon the superficial velocity of vapor leaving the system. This technique, however, is subject to limitations of the pool shape, choice of pool liquids (particularly in connection with Prandtl number effect) and power densities. On the other hand, it may be argued that the circulation patterns and the effective heat transfer coefficients at the pool boundaries are determined by the bubble population characteristics and the pool geometry, and are only weakly influenced by the nature of the gas comprising the bubbles. To test this hypothesis, a series of experiments has been performed in which a permanent gas (air or helium) is injected from a hypodermic tubing network into a pool of the same dimensions as in the Argonne experiments. Heat transfer measurements were made in the horizontal and downward directions as the pool liquid is slowly cooled. By varying the air supply pressure and the orifice diameters and distribution, it is possible to simulate a wide variety of boiling conditions. In addition, one can study heat transfer in non-boiling pools with permanent gas release at the boundaries and interior of the pool. The latter condition would be realized in melting attack of the sacrificial material, particularly concrete. Severe thermal stresses would be expected to cause spalling of the concrete, with detached chips rising in the pool and liberating gas, both from interstitial voids and bound water.

2. Equipment and Procedure

A 6" X 7½" X 6" rectangular pool was constructed of 1/8" brass sheet, with 1/4" copper cooling coils soldered to the outside of the container (Fig. 1).

Cooling (or heating) water could be circulated independently through the coils on both sides and bottom from two constant-temperature baths. An array of pierced stainless steel tubes on 1" centers extending vertically downwards into the pool was used for air injection. The tubing occupied about 0.05% of the cross sectional area and hence offered negligible resistance to circulation. 0.03" diameter holes were drilled through the tubing wall at 1/4" intervals, giving a relatively non-uniform distribution of bubble release sites, which simulated the bubble void fraction distribution in the Argonne boiling experiments. To obtain a much more uniform distribution, the stainless steel tubes were covered by pierced teflon tubing with 0.01" holes covering the drilled holes in the underlying tubing. This resulted in a uniform release site distribution, with small uniform bubbles. The gas (air or helium) flow rate and pressure were measured. The evaporation rate was determined by makeup water additions after a run, as determined by the level in a standpipe. Five thermocouples were embedded in each side wall and in the bottom plate to determine average temperatures in each of these directions. The pool, inlet and outlet water temperatures were also measured by thermocouples. The average heat transfer was determined from the enthalpy gain of the cooling water, while the temperature difference was determined from the average plate temperature and the bulk temperature. Heat balance checks were made periodically, and were generally within 10%. In operation the pool was charged with hot water and heat transfer coeffients determined as the pool cooled down. Most data were taken in the range of 60-80^{o}C.

3. Results

A. Bubble Distribution Effects

Typical data for sideward and downward heat transfer in an air-water system to the pool walls,using the smaller holes (0.01 in.) are shown in Figs. 1 and 2. h_s and h_d appear to be independent of the mean difference between the pool and wall temperatures, but depend upon the gas flow rate. With bare stainless tubing (0.03 in. holes) similar effects were observed, as shown in Figs. 3 and 4, but the heat transfer coefficients were markedly reduced, particularly at the low flow rates. This significant effect can be understood from the spatial and size distribution of bubbles in the two cases. With the smaller sites, all were apparently equally operative, and the bubbles were uniform, small,and rose vertically without coalescence. With the larger holes (.03"), the gas release was primarily in the upper half of the pool, with the void fraction distribution depending upon the total gas flow rate. This simulates fairly closely the behavior of the boiling pool, in which at low power the bottom half of the pool is virtually bubble free, but where the lower boundary of the bubbly region moves downwards as the power is increased, so that eventually the entire pool is in bubbly flow. The reduction in uniformity of bubble release has the effect of reducing the average heat transfer coefficient to the sidewalls, primarily because of the reduced liquid circulation. However, even with non-uniform gas bubbles, coalescence and growth are both quite small, which differs markedly from the boiling case. In particular, in boiling experiments the bubbles grow very rapidly, indicating appreciable

superheat, and the large bubbles coalesce rapidly with neighboring small bubbles, in view of their larger rise velocities. Hence, there is virtually a vapor bypass near the top of the pool, with much of the vapor being relatively ineffective in dragging liquid upwards from the bottom of the pool. This will be shown later in comparisons of the present data with the boiling pool data taken at Argonne.

B. Sensitivity to Sidewall Gap Width

Figs. 3, 5 and 6 show the effect of the gap width between the tube bundle and the sidewall. It is seen that at the higher gas flows the heat transfer coefficient is rather satisfyingly independent of gap thickness over the range of 0.25" - 3.25", although at the lowest gas flow, the heat transfer is markedly increased by going to a small gap. This indicates that once vigorous agitation has been established, the sidewall boundary layer thickness is fairly independent of the location of the nearest gas release site, providing that the gap width is large compared to the fully-developed thermal boundary thickness.

C. Injected Gas Density

Some tests were run with helium using bare stainless tubing, as shown in Figs. 7 and 8. On comparing with Figs. 3 and 4, it is seen that the heat transfer coefficient is practically independent of the gas density. This is not particularly surprising, since the gas-liquid density ratio does not effectively determine the bubble rise velocity, although it plays an important role in flooding and entrainment phenomona. Hence, one might expect that gas density effects might be more significant at very high powers.

D. Comparison with Boiling Pool Data

In order to make a valid comparison with boiling pool data, it was necessary to estimate the total gas volumetric flux, $j_g = j_w + j_a$; where j_w and j_a are the water vapor and air volumetric fluxes, respectively, leaving the pool. This is a function of both the pool temperature and the gas flow rate, as shown in Fig. 9, where the dotted lines refer to the values of j_g/j_a which would be obtained at each temperature if the bubbles leaving the system were saturated with water vapor, and no free surface evaporation took place. Clearly, the free surface evaporation component is significant. To estimate this effect in a boiling pool, one notes that the data in Fig. 9 are correlated by the empirical equation:

$$j_g/j_a = c \ell n \, j_a/j_a^* \qquad (1)$$

where $j_g/j_a = 1$ when $j_a = j_a^*$, and the slope c is a function of the pool temperature. Upon plotting c as a function of the partial pressure driving force for surface evaporation (Fig. 10) and extrapolating to $\Delta p = 760$ mm H_g, one can determine the equivalent exit superficial velocity V_o (or j_g) in a boiling pool. A comparison with the ANL boiling pool data can then be made, as shown in Figs. 11 and 12, where the dotted lines represent the boiling pool data band. It is seen that the non-uniform gas injection data, simulating the peaked void fraction vertical distribution observed in the boiling pool fall within the data bands, both for sideward and downward heat transfer. However, they are still on the high side, in view of the more efficient stirring in

to the sides, so that the development of the pool shape depends markedly on nucleation aspects.

List of Figures

References

1. J. D. Gabor, "Heat Removal from Heat-Generating Salt-Water Pools", 2nd Annual Post-Accident Removal Information Exchange Meeting, Nov. 13-14,1975, Albuquerque, NM.

2. R. P. Stein, J. C. Hesson, and W. H. Gunther, "Studies in Heat Removal from Heat Generating Boiling Pools," Beverly Hills ANS Meeting, 1974.

3. J. D. Gabor, L. Baker, Jr., R. P. Stein, J. C. Cassulo, and W. H. Gunther "Heat Removal from Heat Generating Pools", Washington ANS Meeting, 1974.

FIG. 1

SIDE 1, AIR, UNIFORM SITES

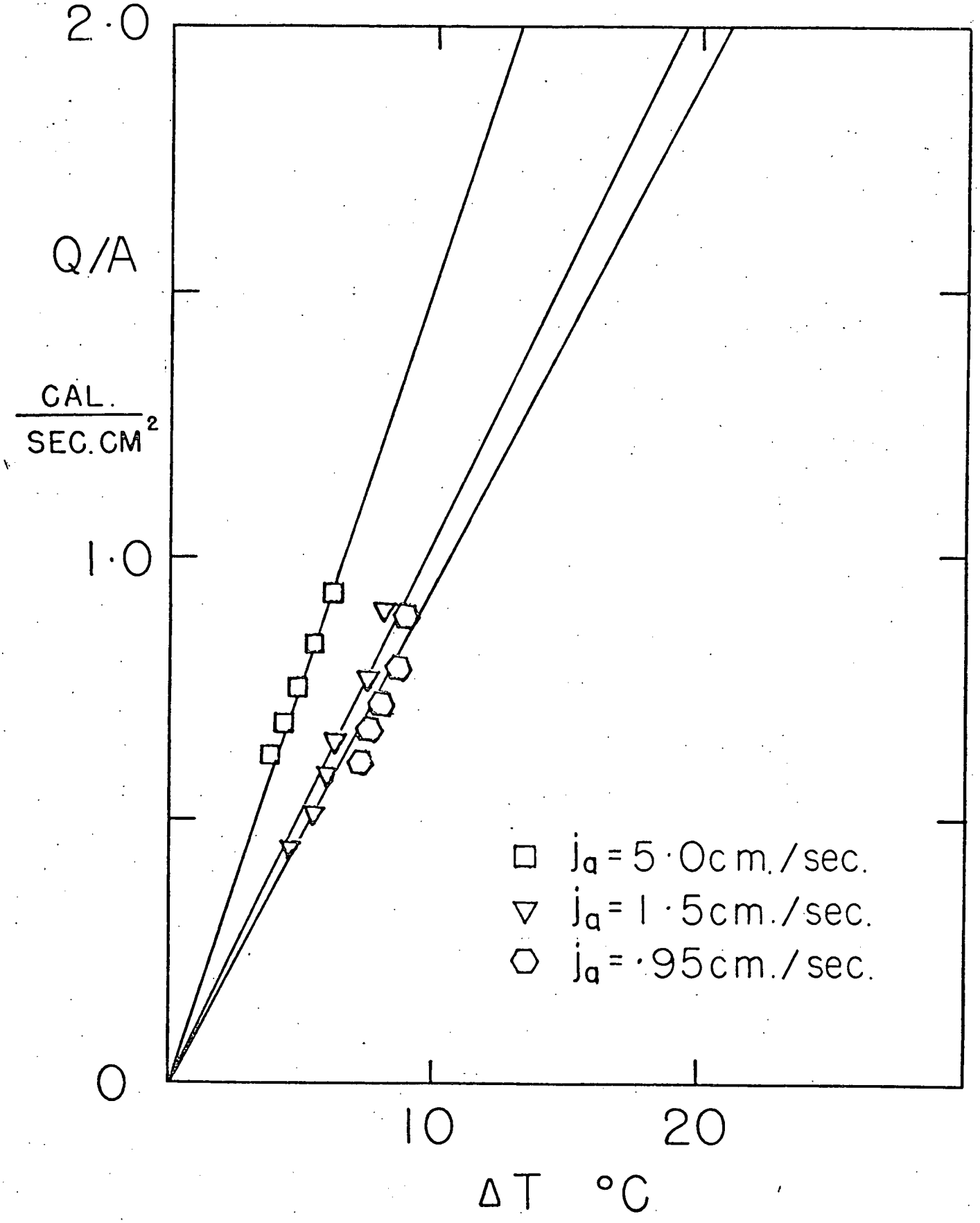

FIG. 2

BOTTOM, AIR, UNIFORM SITES

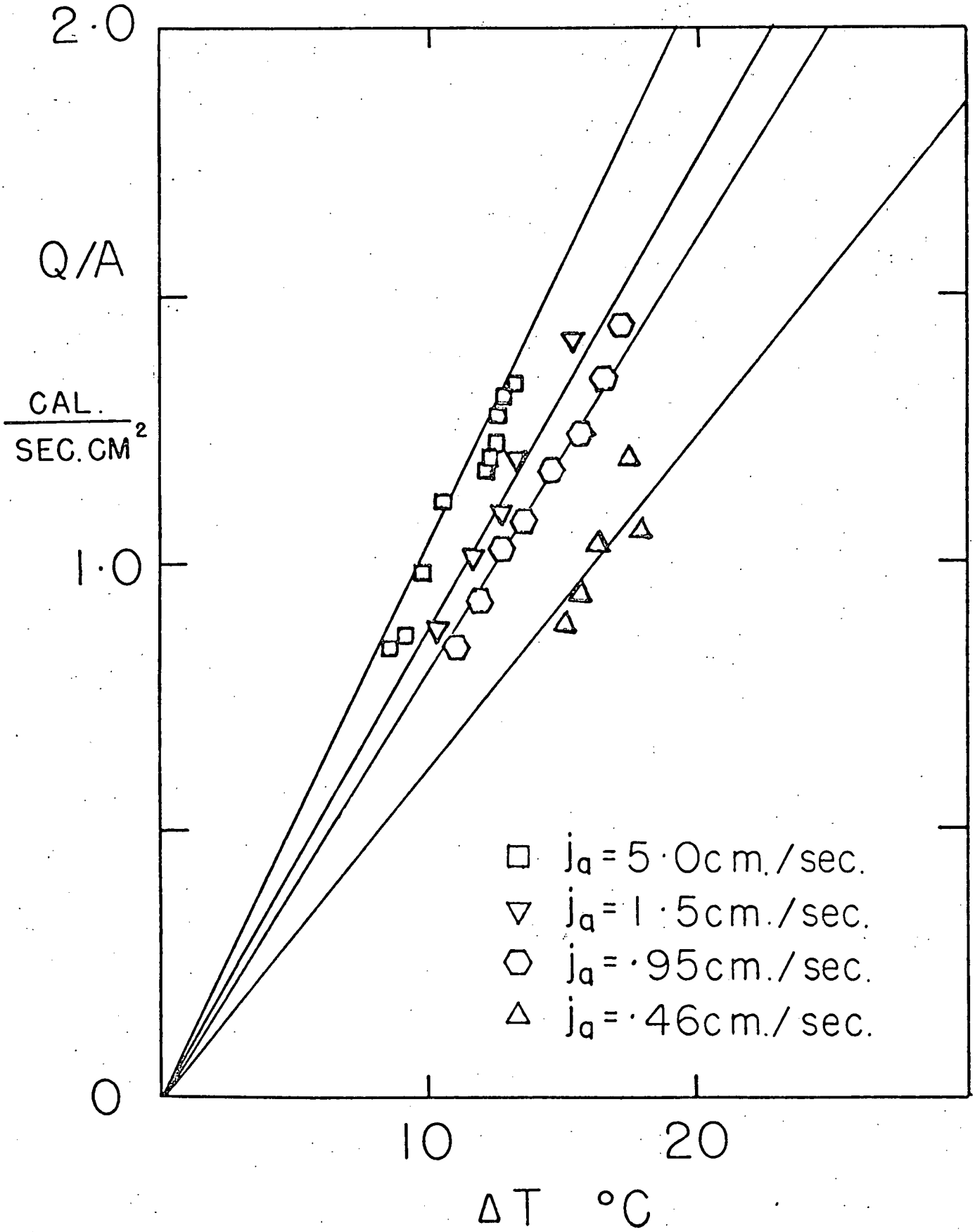

FIG. 3

SIDE 1, AIR, X = 1·75"

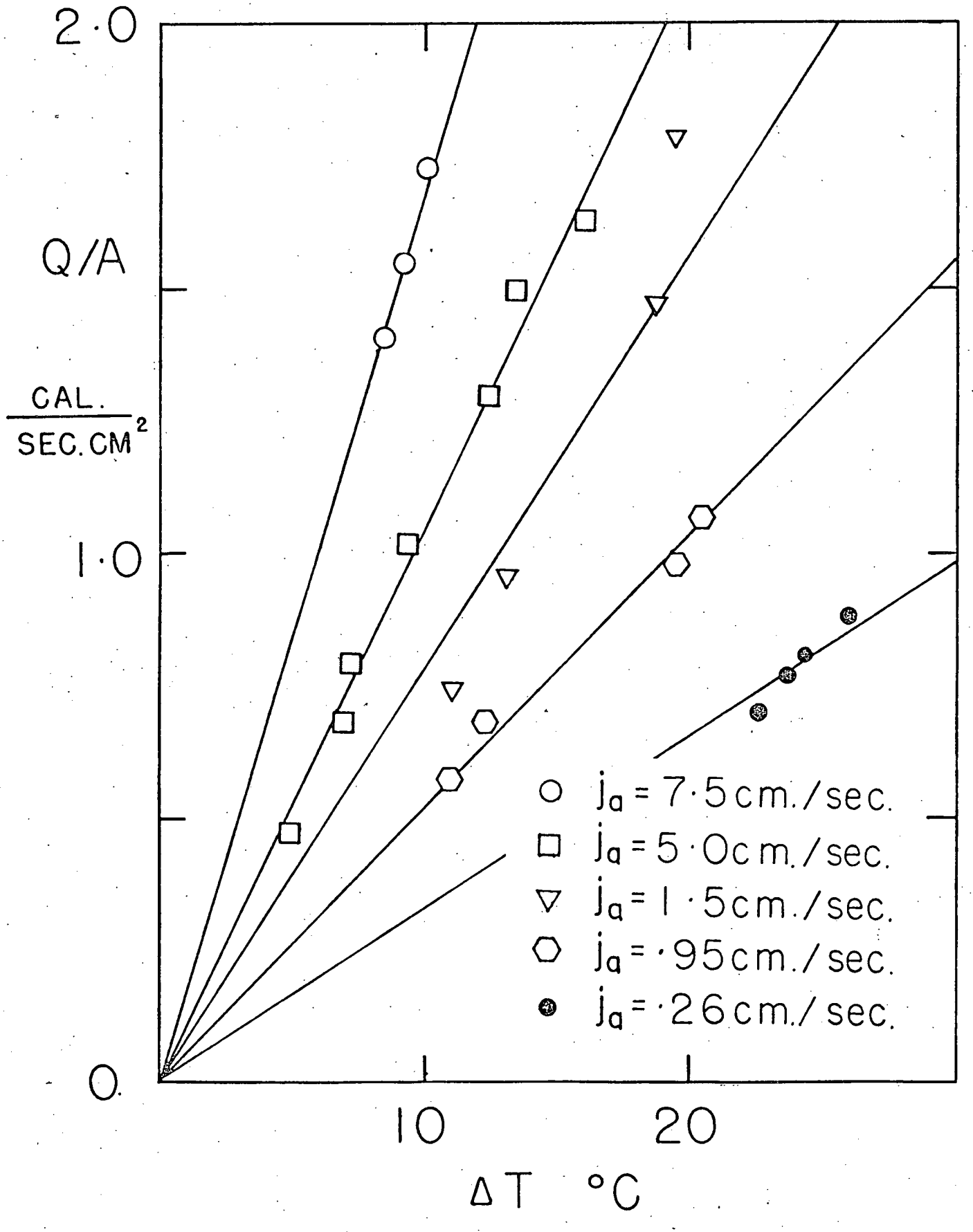

FIG. 4

BOTTOM, AIR

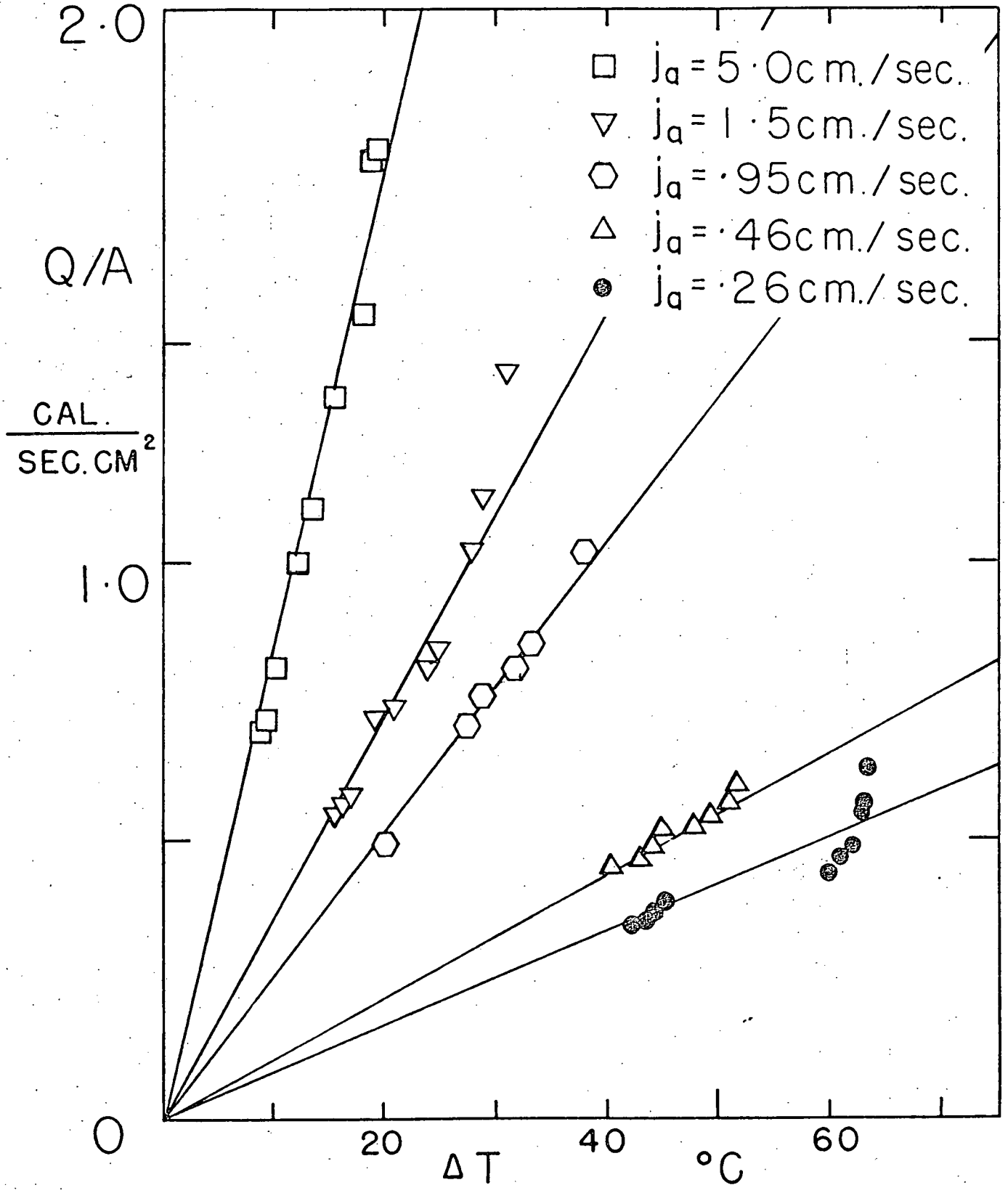

FIG. 5

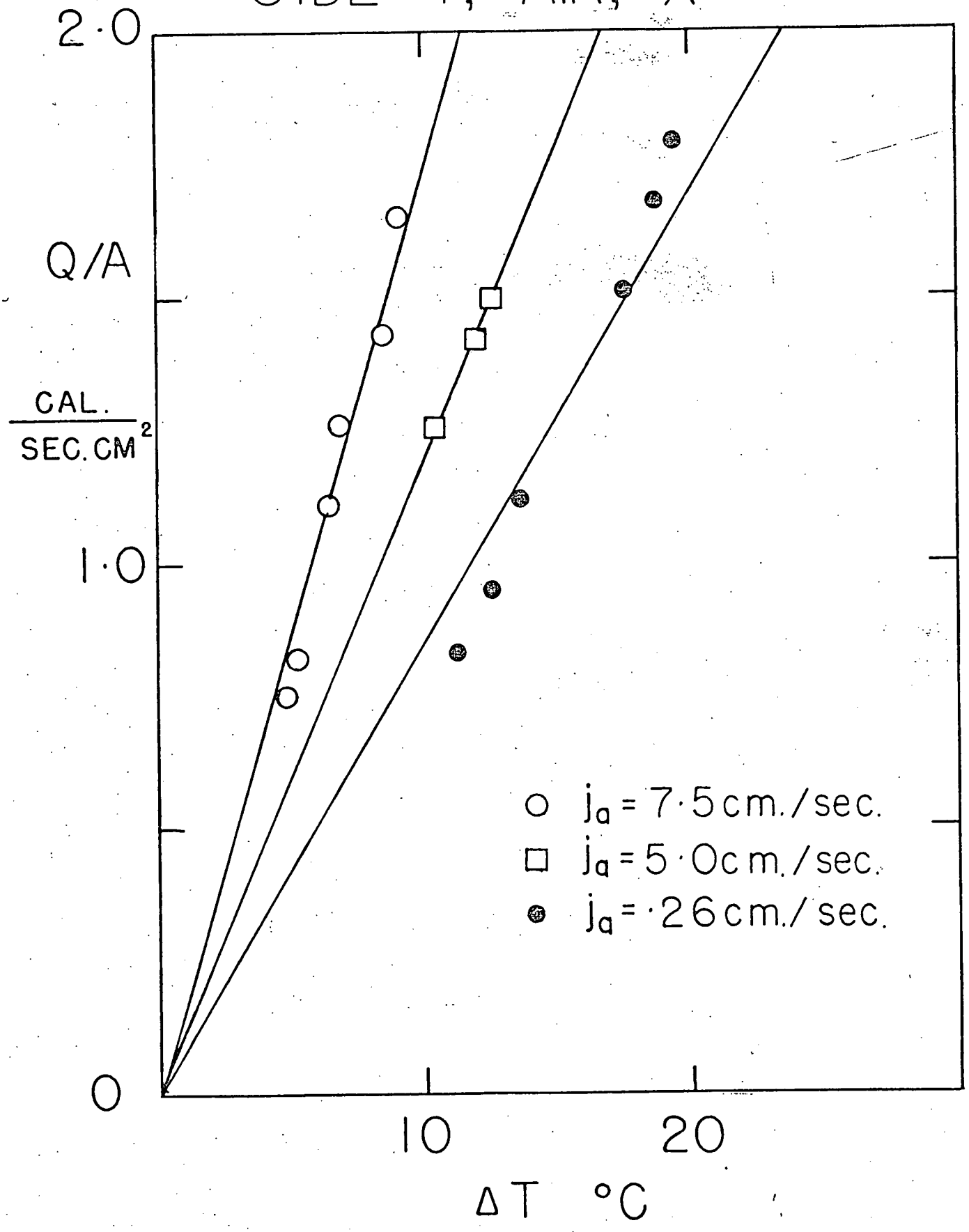
SIDE 1, AIR, X = 1/4"
2·0
Q/A
CAL./SEC.CM²
1·0
0
10
20
ΔT °C
○ j_a = 7·5 cm./sec.
□ j_a = 5·0 cm./sec.
● j_a = ·26 cm./sec.

FIG. 6

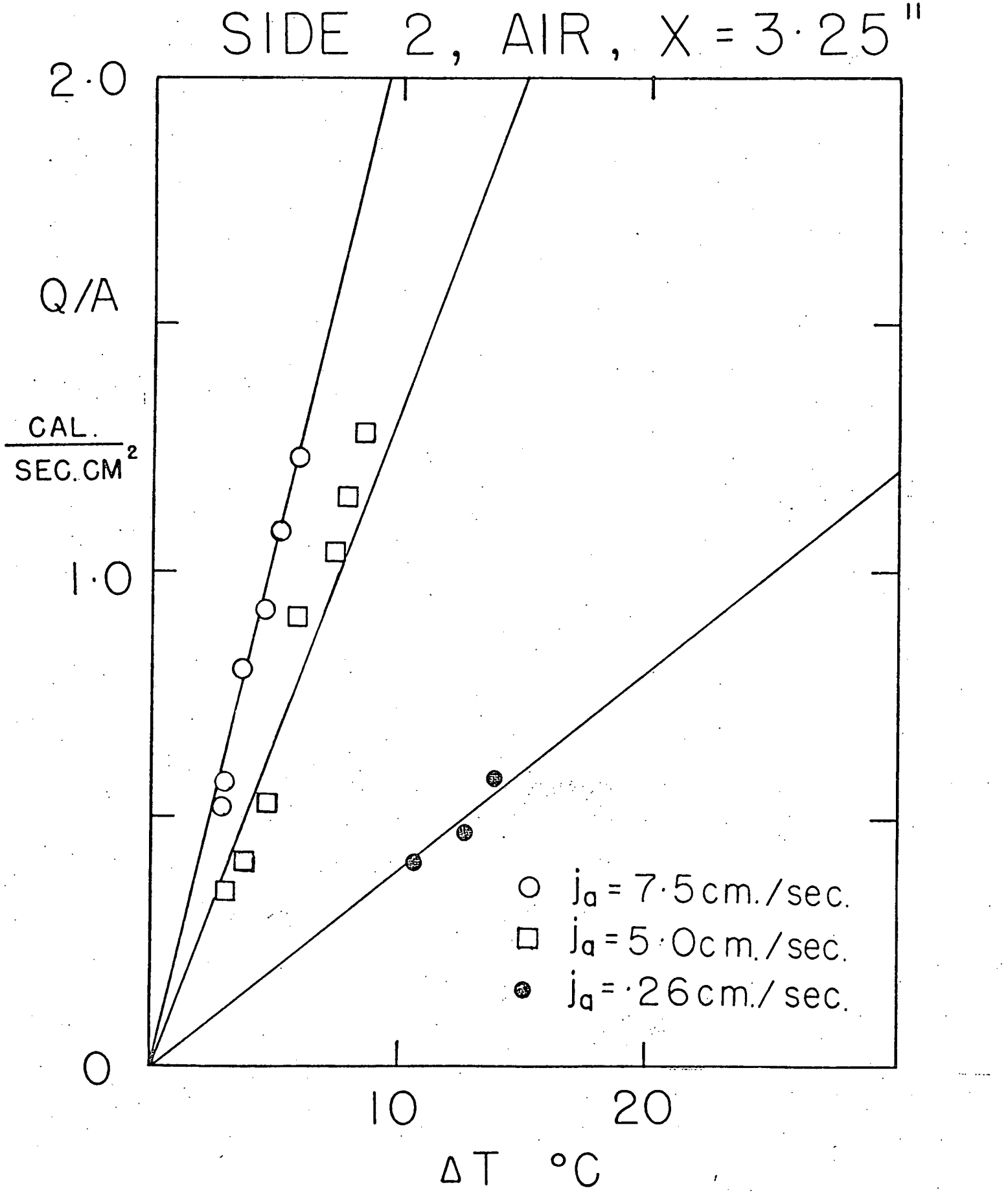
SIDE 2, AIR, X = 3·25"
2·0
Q/A
CAL./SEC.CM²
1·0
0
10
20
ΔT °C
○ j_a = 7·5 cm./sec.
□ j_a = 5·0 cm./sec.
● j_a = ·26 cm./sec.

FIG. 7

SIDE 1, He, X = 1·75"

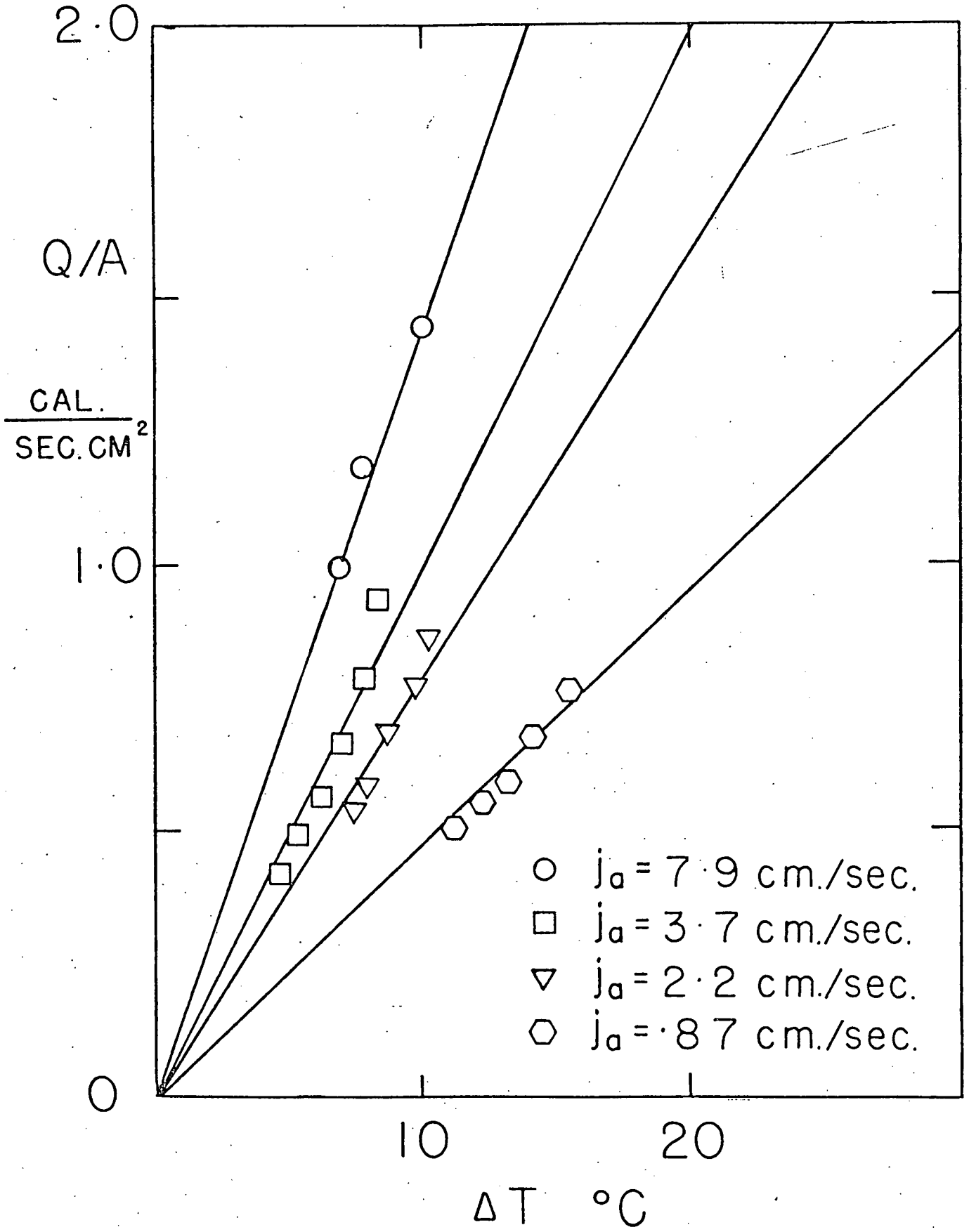

FIG. 8

BOTTOM, He

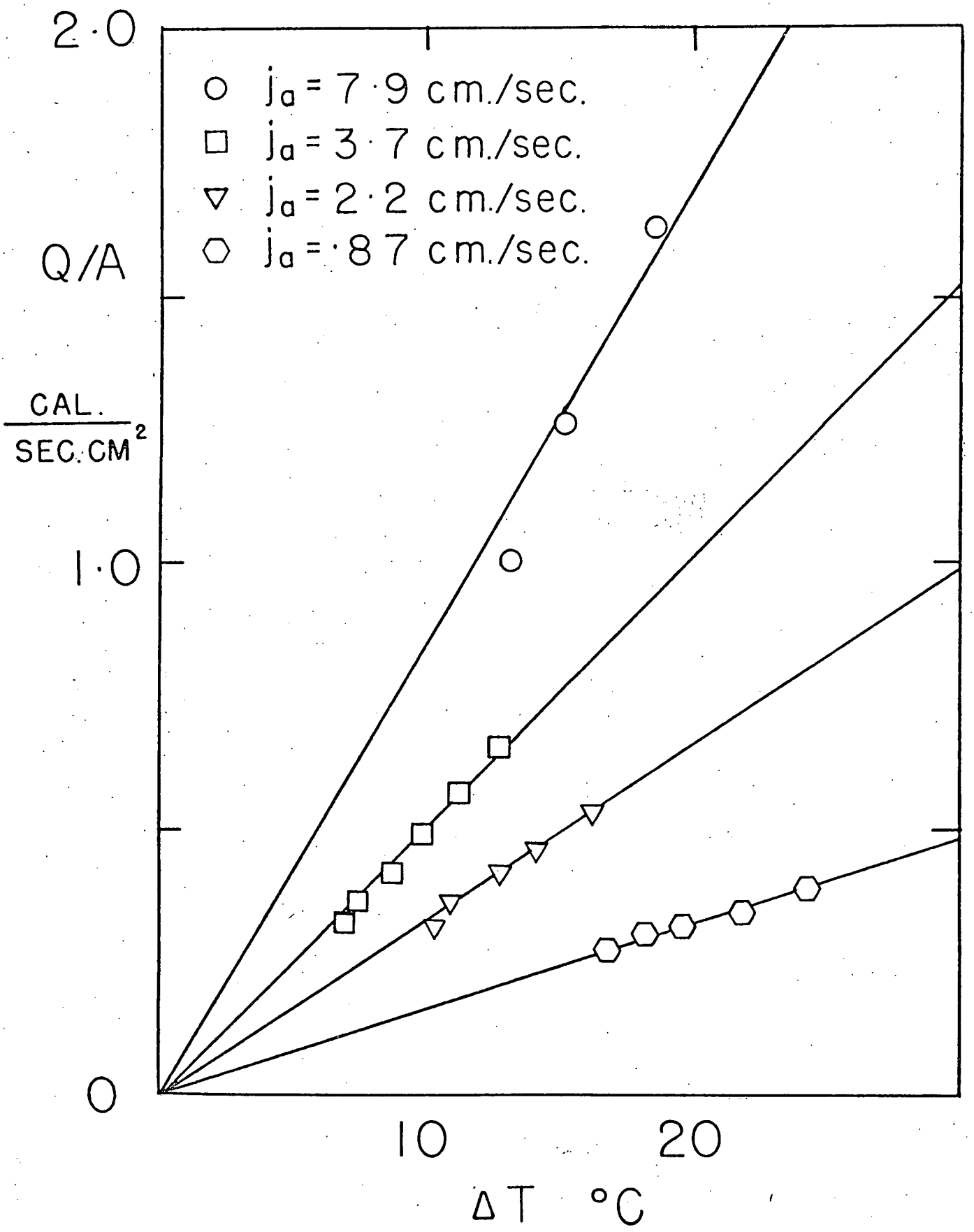

FIG. 9

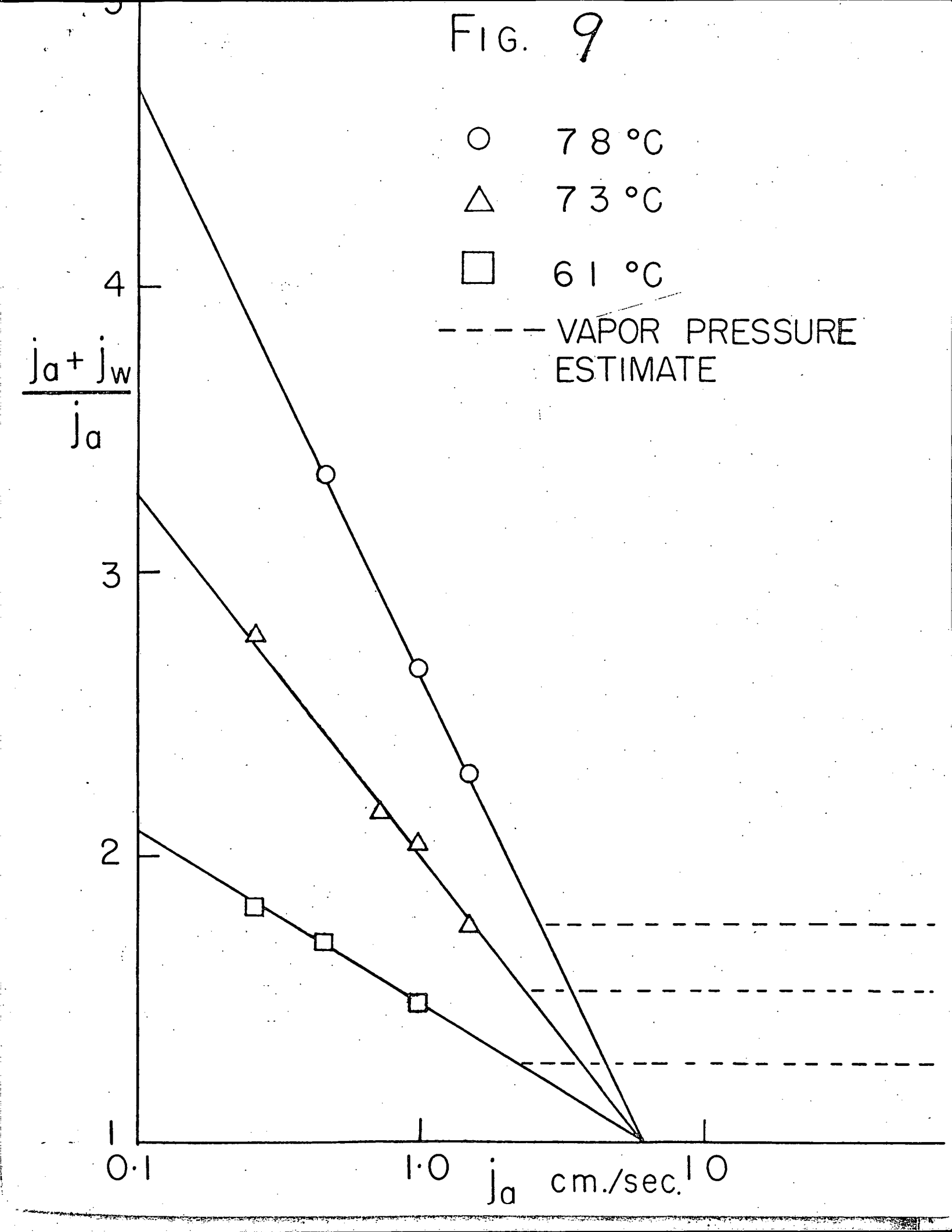
78 °C
73 °C
61 °C
VAPOR PRESSURE ESTIMATE
$\frac{j_a + j_w}{j_a}$
4
3
2
1
0·1
1·0
10
j_a cm./sec.

FIG. 10

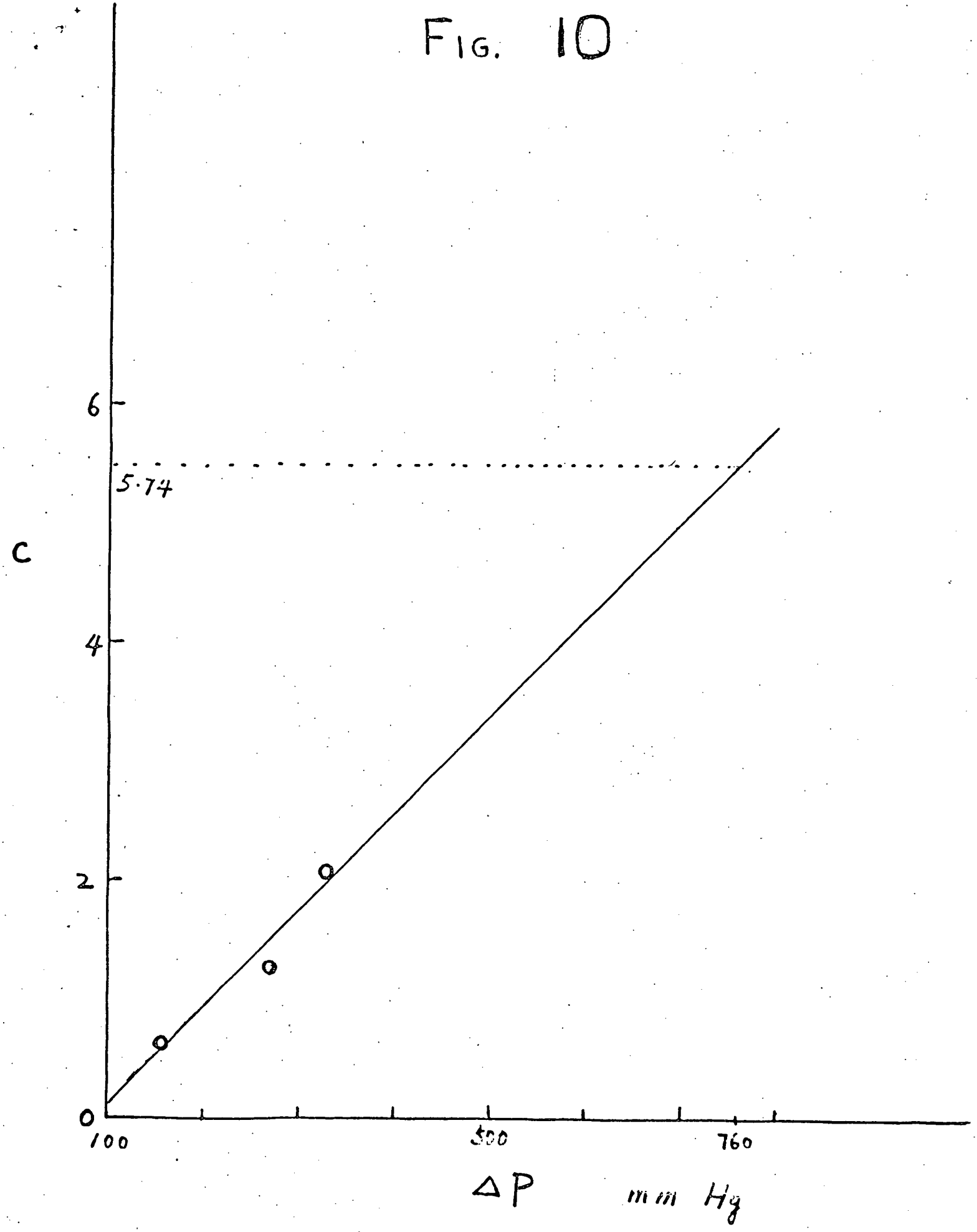

FIG. 11

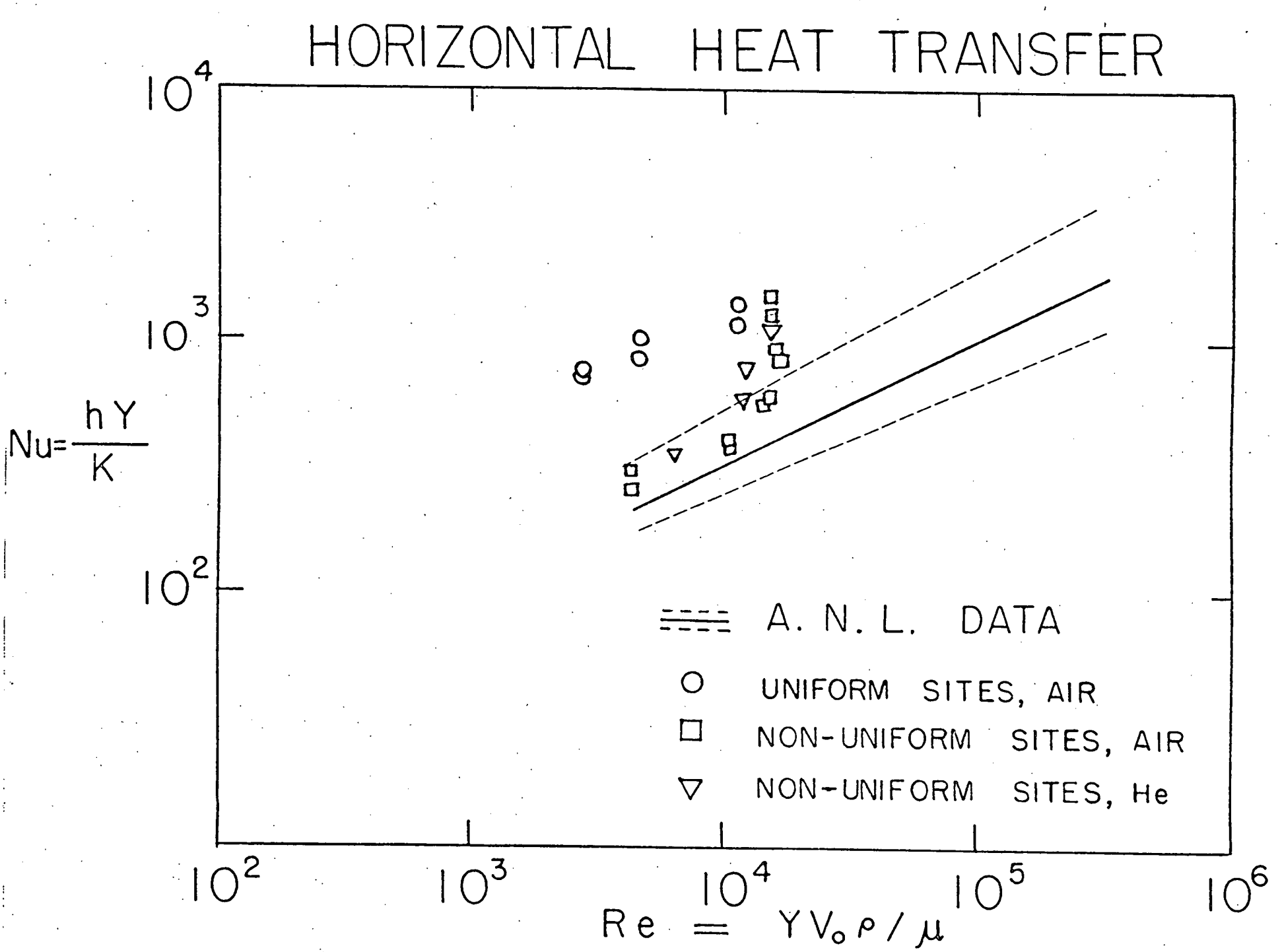
HORIZONTAL HEAT TRANSFER
10^4
10^3
10^2
$Nu = \frac{hY}{K}$
A. N. L. DATA
UNIFORM SITES, AIR
NON-UNIFORM SITES, AIR
NON-UNIFORM SITES, He
10^2
10^3
10^4
10^5
10^6
$Re = YV_o\rho/\mu$

FIG. 12

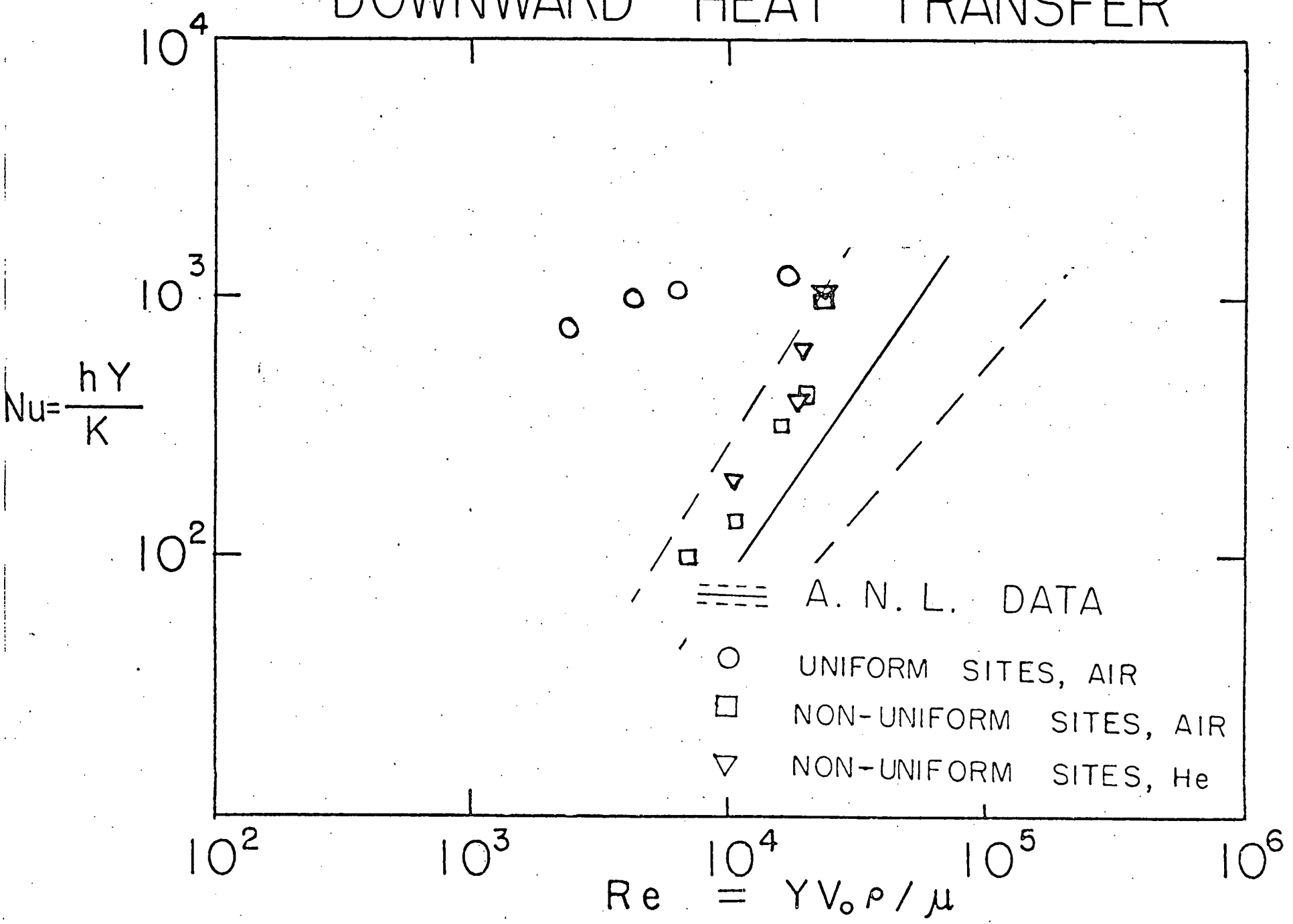
DOWNWARD HEAT TRANSFER
10^4
10^3
10^2
$Nu = \frac{hY}{K}$
A. N. L. DATA
UNIFORM SITES, AIR
NON-UNIFORM SITES, AIR
NON-UNIFORM SITES, He
10^2
10^3
10^4
10^5
10^6
$Re = YV_o\rho/\mu$

FIG. 13

OIL

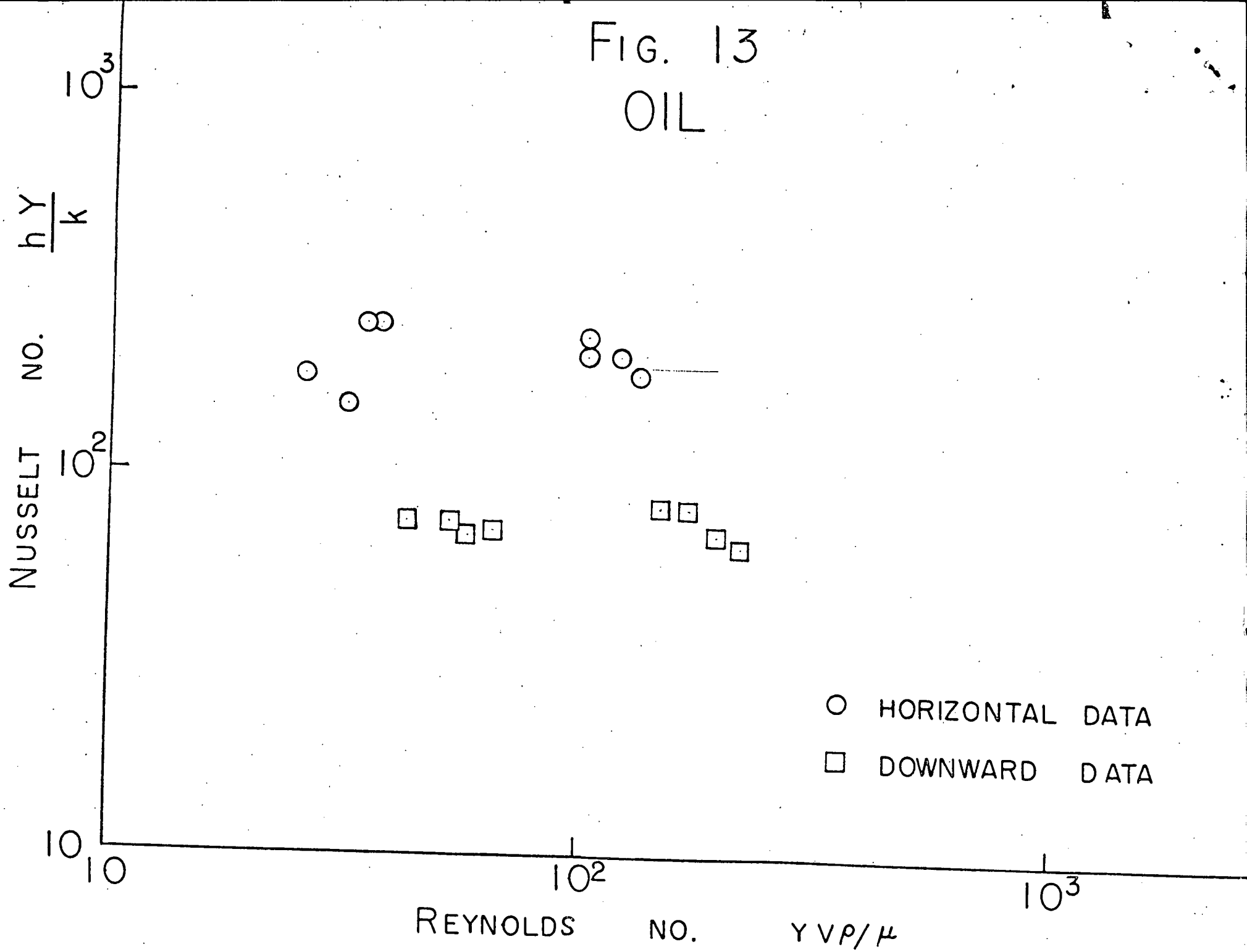
NUSSELT NO. $\frac{hY}{k}$
10^3
10^2
10^1
10^1
10^2
10^3
REYNOLDS NO. $YV\rho/\mu$
HORIZONTAL DATA
DOWNWARD DATA